

Oligonary Nitrides and Oxonitrides of Si, P, Al, and B in Combination with Rare Earth or Transition Metals as well as Molecular Precursor Compounds with Nitrido Bridges M-N-Si (M = Ti, Zr, Hf, W, Sn).

Wolfgang Schnick*, Regina Bettenhausen, Brigitte Götze, Henning A. Höpfe, Hubert Huppertz, Elisabeth Irran, Klaus Köllisch, Rainer Lauterbach, Michael Orth, Stefan Rannabauer, Thomas Schlieper, Bernd Schwarze, Frank Wester

München, Department Chemie der Ludwig-Maximilians-Universität

Abstract. A novel synthetic approach is presented leading to hitherto unknown nitridosilicates, oxonitridosilicates, oxonitridoaluminosilicates, carbidonitridosilicates, as well as nitridoborates and oxonitridoborates of rare earth elements, alkali, and alkaline earth metals. Typically, the respective metals were reacted with silicon diimide, aluminum nitride, or poly(boron amide imide), respectively, under pure nitrogen atmosphere utilizing a radiofrequency furnace. Usually, the compounds are obtained within short reaction periods as coarsely crystalline products. Zinc nitridophosphates of the sodalite structure type were obtained by the reaction of phosphorus

nitride imide with zinc or zinc chalcogenides, respectively. Several molecular metal silylamides and imides containing nitridobridges between the metals and silicon were obtained by the reaction of differently chlorinated disilazanes with metal chlorides. During these investigations hitherto unknown bis(trimethylsilyl)ammonium salts have been discovered. Furthermore, we report about the synthesis of N-silyl metal hydrazides.

Keywords: Nitrides; Nitrido bridges; Oxonitrides

Oligonäre Nitride und Oxonitride von Si, P, Al und B mit Seltenerd- bzw. Übergangsmetallen sowie molekulare Vorläuferverbindungen mit Nitridobrücken M-N-Si (M = Ti, Zr, Hf, W, Sn)

Inhaltsübersicht. Es wurde ein neues Verfahren zur Synthese von Nitridosilicaten, Oxonitridosilicaten, Oxonitridoaluminosilicaten, Carbidonitridosilicaten sowie Nitridoboraten und Oxonitridoboraten der Seltenerd-, Erdalkali- bzw. Alkalimetalle entwickelt, bei dem die entsprechenden Metalle mit Siliciumdiimid bzw. Aluminiumnitrid oder Boramidimid im Hochfrequenzofen unter Stickstoff-Atmosphäre umgesetzt wurden. Die Produkte entstehen dabei in kurzen Reaktionszeiten zumeist in grobkristalliner Form. Zink-ni-

tridophosphate vom Sodalith-Strukturtyp wurden durch Umsetzung von Phosphornitridimid mit Zink bzw. Zinkchalcogeniden erhalten. Verschiedene molekulare Metall-silylamide und -imide mit Nitridobrücken zwischen den Übergangsmetallen und Silicium wurden durch Umsetzung unterschiedlich chlorierter Disilazane mit Metallchloriden erhalten. Bei diesen Reaktionen wurden zuvor unbekannte Bis(trimethylsilyl)ammonium-Salze entdeckt. Daneben wird auch über N-Silylmetallhydrazide berichtet.

Introduction

Polymeric nonmetal nitrides are of considerable interest for the development of inorganic materials for high-performance applications [1, 2]. Among the binary members of this class of compounds cubic and hexagonal boron nitride (BN) as well as silicon nitride (Si_3N_4) increasingly have gained relevance. Practical applications include substrates for semiconductors on the basis of Si_3N_4 or high-temperature materials like valve tappets and turbochargers (Si_3N_4) or crucibles made of hexagonal BN [1].

The binary compounds BN and Si_3N_4 are well-known since the last century. However, both nitrides have not previously been used as starting materials for the synthesis of oligonary nonmetal nitrides. A varied chemistry comparable to that of oxidic borates, silicates, or phosphates, which derives by formal exchange of oxygen by nitrogen, has not been established until recently [1]. However, the numerous oxidic silicates and phosphates, which include the clay minerals or the framework structures of zeolites illustrate the demand for multinary nitrides in the systems M-Si-N, M-B-N, and M-P-N (M = metal) in order to design novel tailor-made materials.

Oligonary nitrides and oxonitrides of Si, P, Al, and B

The most important reason for the lack of knowledge concerning multinary nitrides of Si, P, Al, or B was the high chemical and thermal stability of the respective binary ni-

* Prof. Dr. W. Schnick
Department Chemie
Ludwig-Maximilians-Universität München
Butenandtstraße 5 – 13 (D)
D-81377 München, Germany
Fax: +49-(0)89-2180-77440
E-Mail: wolfgang.schnick@uni-muenchen.de

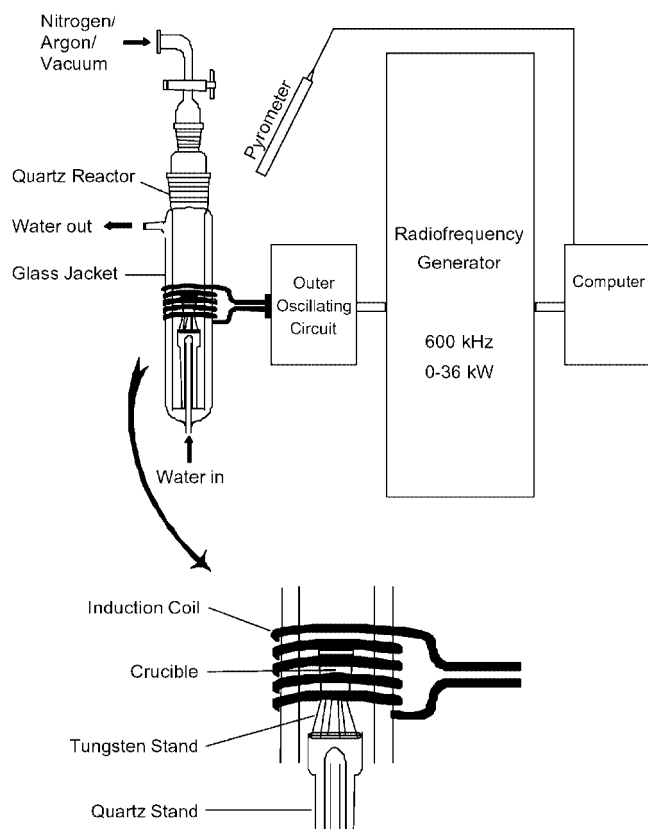


Fig. 1 Radiofrequency furnace for the syntheses of nitridosilicates, sions, and sialons.

trides (e.g. Si_3N_4 , AlN , and BN). On one hand this inertness is an important precondition for an application of these nitrides as materials in high-temperature and high-performance devices. On the other hand this property seems to rule out their utilization as starting materials in chemical reactions.

Oxidic silicates are accessible by high-temperature reactions of silica (SiO_2) with metal oxides or carbonates. However, an analogous broad synthetic approach seems to be difficult for nitridosilicates and other related nonmetal nitrides. And even the hydrothermal method, which represents an important synthetic tool for the preparation of oxidic zeolites, could not as yet be adapted and modified to an analogous ammonothermal route leading to nitridosilicates. For these reasons we have developed an optimized synthetic approach leading to ternary and multinary nitridosilicates by high-temperature reactions of pure metals with silicon diimide. With this broad synthetic access several novel nitridosilicates have been obtained and characterized.

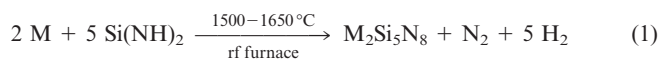
Synthetic procedure

For the syntheses of nitridosilicates and the related oxonitridosilicates a specially developed computer controlled radiofrequency (rf) furnace is used for the inductive heating of the crucibles [3, 4].

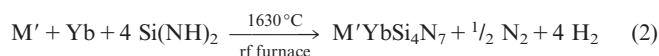
Experimental set-up: The crucible which contains the reaction mixture is positioned on a tungsten stand inside a water cooled quartz reactor (Fig. 1). The reactor is surrounded by a water cooled induction coil wherein the crucible is centered. The induction coil is connected to a radiofrequency generator (type: IG 30-400, Hüttinger, Freiburg, Germany) via the outer oscillating circuit. The input power of the generator amounts to a voltage of 380 V (AC) with a maximum current strength of 3×120 A. The power output was 0–36 kW with an effective maximum voltage of 7000 V. The optimum working frequency depends on the crucible material and the gas atmosphere in the quartz reactor. For the selection of the crucible materials (e.g. tungsten, tantalum, graphite) specific properties like the chemical inertness and the electronic conductivity at high temperatures were considered. For tungsten crucibles in an argon atmosphere a working frequency of 600 kHz is used. The energy transfer from the coil to the crucible is relatively poor (coupling constant: 0.28). This is due to the spatial separation in our experimental set-up (diameter of the tungsten crucible: 24 mm, induction coil: 72 mm). Optimized tuning of the resonant cycle yields a maximum temperature of 2350 °C with tungsten crucibles and above 3000 °C with graphite crucibles. For the thermal control of the crucible an external pyrometer is used. For reactions during which metals evaporate and condense on the inner surface of the quartz reactor power controlled temperature programs based on calibration curves obtained with empty crucibles are used. The quartz reactor is connected to a vacuum line and an inert gas supply (Ar , N_2). With this experimental set-up fast heating rates (500 °C/min) but also quenching of the reaction products are possible.

Synthesis of nitridosilicates, oxonitridosilicates, and sialons:

The novel synthetic approach, abandoning the use of the binary nitrides and treating the pure metals with silicon diimide ($\text{Si}(\text{NH})_2$) instead, proved to be successful for the synthesis of several nitridosilicates [Eq. (1) and (2)].



$\text{M} = \text{Ca}, \text{Sr}, \text{Ba}, \text{Eu}$



$\text{M}' = \text{Sr}, \text{Ba}, \text{Eu}$

Silicon diimide $\text{Si}(\text{NH})_2$ is an amorphous and relatively undefined but reactive compound which converts to amorphous Si_3N_4 at temperatures above 900 °C. It is an important precursor for the technical production of Si_3N_4 ceramics [5]. Silicon diimide $\text{Si}(\text{NH})_2$ is obtained in preparative amounts by ammonolysis of SiCl_4 followed by thermal treatment at 600 °C [Eq. (3)].



The reactions between a metal and $\text{Si}(\text{NH})_2$ [Eq. (1) and (2)] may be interpreted as a dissolution of electropositive metals in the nitrido analogous, polymeric acid $\text{Si}(\text{NH})_2$, accompanied by the evolution of hydrogen. Basically, several metals with melting points below 1600 °C can be used for this procedure. Similarly to the formation of Si_3N_4 whiskers a vapor-solid (VS) [6], a vapor-liquid-solid (VLS) [7], or

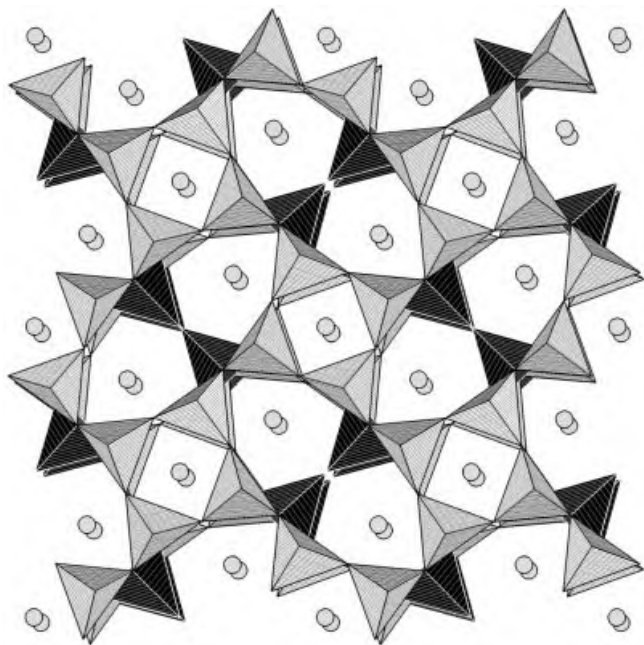


Fig. 2 Crystal structure of $M'_3\text{Si}_6\text{N}_{11}$ ($M' = \text{Ce}, \text{Pr}$).

a liquid-solid (LS) mechanism is assumed for the synthesis of nitridosilicates. The nitridosilicates are accessible as coarsely crystalline, single-phase products in short reaction times in preparative amounts with metals melting at approximately 1000 °C. Depending on the molar ratio of metal and silicon diimide in the starting mixture highly cross-linked or lower condensed nitridosilicates are produced.

In the meantime we extended our synthetic attempts to nitridoaluminosilicates and compounds in the system Si-Al-O-N as well. These oxonitridoaluminosilicates (sialons) are built up from corner-sharing (Si,Al)(O,N)₄ tetrahedra and they derive from the nitridosilicates by formal substitution of Si by Al and N by O. However, due to kinetic reasons such substitutions do not seem to be possible starting from pure nitridosilicates or oxosilicates. Due to its specific thermal behavior SrCO₃ is a useful starting material for the synthesis of oxonitridosilicates. For the synthesis of the respective aluminonitridosilicates we added AlN.

Nitridosilicates and carbidonitridosilicates

Highly condensed network structures of corner sharing SiN₄ tetrahedra previously have been identified in our group, namely the alkaline earth compounds M₂[Si₅N₈] ($M = \text{Ca}, \text{Sr}, \text{and Ba}$ [8]). In the meantime we have extended this synthetic approach to rare-earth nitridosilicates and we obtained $M'_3[\text{Si}_6\text{N}_{11}]$ with $M' = \text{Ce}, \text{Pr}$ (Fig. 2) [9] as well as BaEu(Ba_{0.5}Eu_{0.5})YbSi₆N₁₁ [10]. Though both nitridosilicates have an identical molar ratio Si : N, the topology of the respective [Si₆N₁₁]⁹⁻ substructures significantly differs (cycle-class sequences of the [Si₆N₁₁]⁹⁻ substructures: M₃Si₆N₁₁ {-,0,4,2,0,24,40...}, BaEu(Ba_{0.5}Eu_{0.5})YbSi₆N₁₁ {-,0,11,4,6,8,4...}).

The first nitridosilicate with a divalent rare earth metal was Eu₂[Si₅N₈], which is isotopic with Sr₂[Si₅N₈] and Ba₂[Si₅N₈] [11]. Magnetic susceptibility measurements of Eu₂Si₅N₈ show Curie-Weiss behavior above 50 K with an experimental magnetic moment of 7.67(5) μ_B/Eu indicating Eu²⁺. Ferromagnetic ordering is detected at a remarkably high temperature of 13.0(5) K. The two crystallographically independent Eu²⁺ sites could not be distinguished by ¹⁵¹Eu Mössbauer spectroscopy. The room temperature spectrum has been fitted by only one signal at an isomer shift of δ = -11.82(5) mm/s subject to quadrupole splitting of ΔE_Q = 16.8(2) mm/s and an asymmetry parameter of 0.67(7). At 4.2 K full magnetic hyperfine field splitting is observed with a hyperfine field of 24.9(2) T at the Eu nuclei [12]. In detail we investigated the optical properties of the solid solution series Ba_{2-x}Eu_xSi₅N₈ (0.14 ≤ x ≤ 1.16), which exhibit a very shining orange color [13]. Excitation with intense laser light at 1047 nm reveals fluorescence emission peaking at ~ 600 nm due to two-photon-excitation. The emission maximum is shifted towards higher wavelengths with increasing Eu²⁺ content. Two neighboring maxima in the emission spectrum could be correlated with the two crystallographically independent Eu²⁺ sites, whose coordination by the nitrogen atoms of the [Si₅N₈]⁴⁻ substructure slightly differs. In Ba_{1.89}Eu_{0.11}Si₅N₈ a long lasting luminescence (< 15 min) was observed. This effect is due to the recombination of holes and traps consisting of nitrogen vacancies formed by the reducing synthesis conditions. The maximum emission was observed at -7 °C [13].

A simple measure for the degree of condensation in both oxo- and nitridosilicates (which are built up by connected SiX₄ tetrahedra (X = O, N)) is the molar ratio Si : X. The degree of condensation may vary in a wider range in case of the nitridosilicates (1 : 4 ≤ Si : N ≤ 3 : 4), while oxosilicates (1 : 4 ≤ Si : O ≤ 1 : 2) only have terminal O^[1] and simply bridging O^[2]. In accordance with the higher degree of condensation also N^[3] have been found for Si : N > 1 : 2 in the respective nitridosilicates. Each of these N^[3] are bridging three neighboring Si tetrahedral centers. Thus, in many nitridosilicates the cross-linking at the X atoms and the degree of condensation is enhanced as compared to oxosilicates. Most of these Si-N network structures have no structural analogues among the oxosilicates. According to simple bond-valence considerations, the contribution of the nitrogen atoms towards coordination of the electropositive metal cations decreases as N^[2] > N^[3], with the ammonium type N^[4] exhibiting no contribution at all.

Even for a very high molar ratio Si : N a further increase of the cross-linking at the nitrogen atoms yielding N^[4] bridges was not expected to be possible. Even in binary Si₃N₄ this situation does not occur. Surprisingly the quaternary compounds MYbSi₄N₇ (M = Sr, Ba, Eu) exhibit such unusual N^[4] bridges (Fig. 3) [14].

All previously described nitridosilicate network structures are built up from alternating Si and N, with the nitrogen atoms being negatively polarized. In contrast the unprecedented structural motif NSi₄ in the quaternary com-

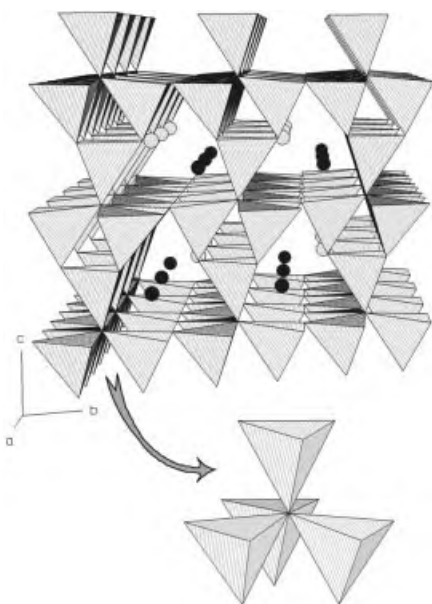


Fig. 3 Crystal structure of MYbSi_4N_7 ($M = \text{Sr, Ba, Eu}$).

pounds MYbSi_4N_7 ($M = \text{Sr, Ba, Eu}$) exhibits an ammonium character and thus the $\text{N}^{[4]}$ atoms carry a formally positive charge. It seems promising to replace the fourfold coordinated nitrogen atoms by carbon in order to introduce carbon bridges into nitridosilicate network structures. This substitution could lead to better mechanical properties because of the higher covalence of the $\text{Si}-\text{C}$ bond as compared with $\text{Si}-\text{N}$. By serendipity the novel compound $\text{Ho}_2[\text{Si}_4\text{N}_6\text{C}]$ was obtained in very low yield as a byproduct of $\text{Ho}_6[\text{Si}_{11}\text{N}_{20}\text{O}]$ when the synthesis was carried out in graphite crucibles. However, after stoichiometric addition of graphite to the reaction mixture $\text{Ho}_2[\text{Si}_4\text{N}_6\text{C}]$ has been synthesized as a single-phase product. We chose the novel terminus “carbido-nitridosilicate” to emphasize the character of the $\text{Si}^{4+}(\text{N}^{3-}, \text{C}^{4-})$ network, i. e. a substitution of N^{3-} by C^{4-} in nitridosilicates. $\text{Ho}_2[\text{Si}_4\text{N}_6\text{C}]$ consists of a three-dimensional network of star like units $[\text{C}(\text{SiN}_3)_4]$, which are isoelectronic to the characteristic building blocks $[\text{N}(\text{SiN}_3)_4]$ of the above mentioned MYbSi_4N_7 ($M = \text{Sr, Ba, Eu}$) [15]. These blocks are connected sharing their $\text{N}^{[2]}$ atoms to form two types of layers with diametrical orientation of the SiN_3C tetrahedra. Along [001] these two types of layers are alternately connected by further $\text{N}^{[2]}$ atoms like chemical twins (Fig. 4) to build the three-dimensional condensed network $[\text{Si}_4\text{N}_6\text{C}]^{6-}$. As a direct consequence of this chemical twinning the polar character of the $[\text{Si}_4\text{N}_7]^{5-}$ network in $\text{MYb}[\text{Si}_4\text{N}_7]$ is lost. Therefore, $\text{Ho}_2[\text{Si}_4\text{N}_6\text{C}]$ exhibits no SHG activity (second harmonic generation) in contrast to $\text{MYb}[\text{Si}_4\text{N}_7]$.

The nitridosilicates discussed so far show a very high thermal stability (up to 1600 °C) and they are hardly attacked by hot acids and alkalines. Presumably, this is a direct consequence of the high cross-linking in the $\text{Si}-\text{N}$ network structures and its high covalence. However, the question arises, if due to the specific conditions during their

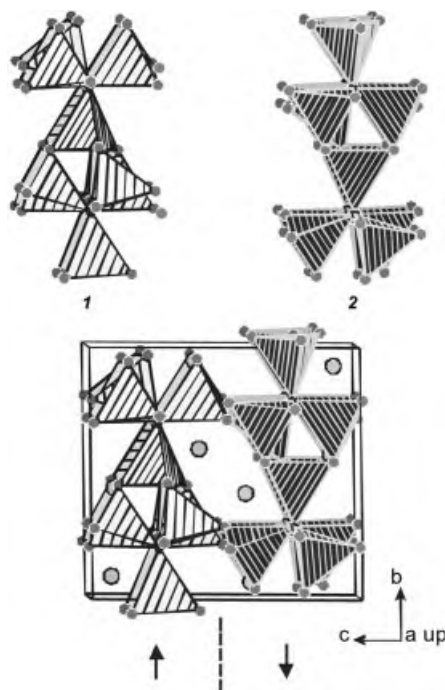


Fig. 4 Crystal structure of $\text{Ho}_2[\text{Si}_4\text{N}_6\text{C}]$, view along [100]. The arrows indicate the diametrical orientation of both layers.

high-temperature syntheses only highly condensed network structures of connected SiN_4 tetrahedra are accessible, or if even less condensed network structures might be possible. It seemed to be specifically challenging also to build zeolite-analogous microporous network structures from SiN_4 tetrahedra. This was achieved with the synthesis of $\text{Ba}_2\text{Nd}_7\text{Si}_{11}\text{N}_{23}$ (Fig. 5). With a molar ratio of $\text{Si} : \text{N} = 11 : 23$ the degree of condensation is smaller than in most oxidic zeolites ($(\text{Al}/\text{Si}) : \text{O} = 1 : 2$). As a consequence terminal $\text{N}^{[1]}$ occur besides simply bridging $\text{N}^{[2]}$. A measure for the microporosity of zeolite analogous structures is the framework density (FD), which indicates the number of tetrahedral centers (T) in a volume of 1000 \AA^3 . With $\text{FD} = 18.5$ $\text{Ba}_2\text{Nd}_7\text{Si}_{11}\text{N}_{23}$ is similar to typical zeolites (FD values for some zeolites: 17.5 ($\text{AlPO}_4\text{-5}$), 17.9 (ZSM-5), 19.3 (No-nasil)) [16].

Nitridoborates

Besides silicon nitride ($\alpha\text{-Si}_3\text{N}_4$, $\beta\text{-Si}_3\text{N}_4$) also binary boron nitride ($h\text{-BN}$, $c\text{-BN}$) plays an important role in the application of non-oxidic high-performance materials [1]. In analogy to the manifold structural chemistry of oligonary nitridosilicates ternary and higher nitridoborates of rare earth elements could be accessible through an analogous synthetic approach. Actually we have been successful to synthesize several nitridoborates utilizing a starting material, namely poly(boron amide imide), which is comparable to silicon diimide $\text{Si}(\text{NH})_2$. Poly(boron amide imide) is an undefined and amorphous but reproducible polymer, that is obtained by ammonolysis of BBr_3 followed by a thermal

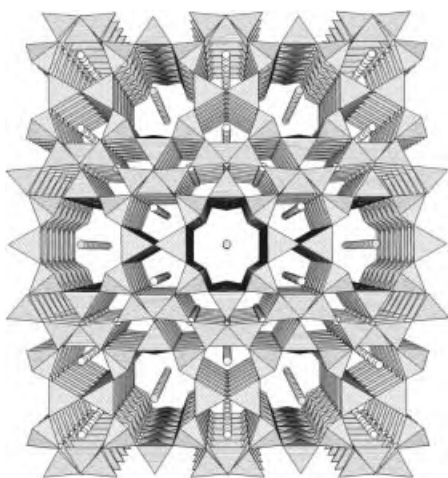


Fig. 5 Crystal structure of $\text{Ba}_2\text{Nd}_7\text{Si}_{11}\text{N}_{23}$, which has a zeolite analogous Si-N framework with wide channels.

condensation below 600 °C. Analogously to the synthesis of the nitridosilicates, we obtained the coarsely crystalline nitridoborate $\text{Pr}_3[\text{B}_3\text{N}_6]$ by the reaction of the pure rare earth metal with poly(boron amide imide) in the radiofrequency furnace under nitrogen atmosphere [17].

All attempts to synthesize an oligonary nitride in the system RE-Si-B-N (RE = rare earth element) by serendipity led to the formation of the novel inclusion compounds $\text{Ba}_4\text{RE}_7[\text{Si}_{12}\text{N}_{23}\text{O}][\text{BN}_3]$ with RE = Pr, Nd, or Sm [18]. According to the single-crystal X-ray diffraction analyses and confirmed by elemental analyses and magnetic investigations these compounds are built up from a network structure of corner sharing SiX_4 tetrahedra (X = N, O) with the oxygen atoms statistically distributed over the X positions. Presumably, oxygen has been incorporated into the product by an oxidic contamination of the rare earth elements. The trigonal planar orthonitridoborate ions $[\text{BN}_3]^{6-}$ and the Ln^{3+} as well are situated in hexagonal cages of the framework. The remaining Ba^{2+} and Ln^{3+} are positioned in channels of the large-pored network structure (Fig. 6).

With respect to a rational planning of the synthesis of microporous nitridozeolites it may be important, that the anions $[\text{BN}_3]^{6-}$ are situated in the $[6^{14}]$ cages of the $[\text{Si}_{12}\text{X}_{24}]$ framework structure. Conceivable though not yet proven is the assumption, that initially during the formation of $\text{Ba}_4\text{Ln}_7[\text{Si}_{12}\text{N}_{23}\text{O}][\text{BN}_3]$ the $[\text{BN}_3]^{6-}$ ions were excised from the boron nitride layers. Subsequently these $[\text{BN}_3]^{6-}$ units do not condense with the nitridosilicate framework but presumably they act as high-temperature stable templates around which the $[\text{Si}_{12}\text{N}_{23}\text{O}]$ framework is organized.

In the meantime we have been successful to extend the described synthetic approach for the preparation of the first oxonitridoborate [19], namely $\text{Sr}_3[\text{B}_3\text{O}_3\text{N}_3]$, and currently we are targeting oxonitridoborates of rare earth elements.

Oxonitridosilicates and oxonitridoaluminosilicates

Nitridosilicates derive from the classical oxosilicates (which are made up of SiO_4 tetrahedra) by a formal exchange of

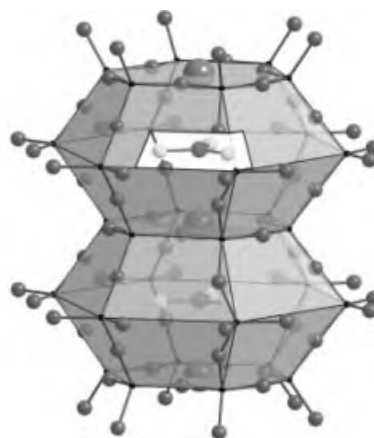


Fig. 6 Crystal structure of $\text{Ba}_4\text{RE}_7[\text{Si}_{12}\text{N}_{23}\text{O}][\text{BN}_3]$ with RE = Pr, Nd, or Sm.

oxygen by nitrogen. Thus they contain SiN_4 tetrahedra. Oxonitridosilicates (so-called “sions”) represent an intermediate class of compounds between oxosilicates and nitridosilicates. A further partial substitution of Si by Al leads to the oxonitridoaluminosilicates (commonly known as sialons). The latter ones exhibit highly desired materials properties like enhanced mechanical hardness and strength, and exceptional thermal and chemical stability. Due to their relevance for the manufacturing and properties of several nitride based ceramic materials they have extensively been studied during the last 30 years [20]. From a structural point of view several sialons derive either from α - or β - Si_3N_4 and therefore they have been called α - or β -sialons, respectively. Other representatives are structurally related to oxidic compounds like melilite (M-phase), apatite (H-phase), or wollastonite (K-phase) [21]. Further novel structure types only rarely had been identified for the sialons. Concerning their solid-state chemistry most of these compounds had been only insufficiently characterized. Detailed structural information was missing as single-crystal diffraction data only for one compound, the so called Nd-U-phase, had been obtained [22]. Within our efforts to investigate compounds comprising nitridobridges between silicon (or aluminum) and rare earth elements (RE) we have particularly focused on oxonitridosilicates and oxonitridoaluminosilicates in order to compare the differing coordination behavior of both the Si-O-RE and Si-N-RE bridges within the same compounds.

Recently, our synthetic strategy utilizing silicon diimide and metals as starting compounds for the synthesis of nitridosilicates in radiofrequency furnaces has been successfully transferred to the synthesis of new oxonitridoaluminosilicates (sialons) and oxonitridosilicates (sions) [23]. Some of these are isotypic with known nitridosilicates, namely $\text{SrSi-Al}_2\text{O}_3\text{N}_2$ [24], $\text{SrErSiAl}_3\text{O}_3\text{N}_4$ [25], or $\text{Nd}_3\text{Si}_5\text{AlON}_{10}$ [26], which are structurally related with LaSi_3N_5 , $\text{BaYbSi}_4\text{N}_7$, and $\text{Ce}_3\text{Si}_6\text{N}_{11}$, respectively. The oxonitrides $\text{Sm}_2\text{Si}_3\text{O}_3\text{N}_4$ and $\text{RE}_2\text{Si}_{2.5}\text{Al}_{0.5}\text{O}_{3.5}\text{N}_{3.5}$ with RE = Ce, Pr, Nd, Sm, Gd [27] belong to the melilite structure type, and the sialons

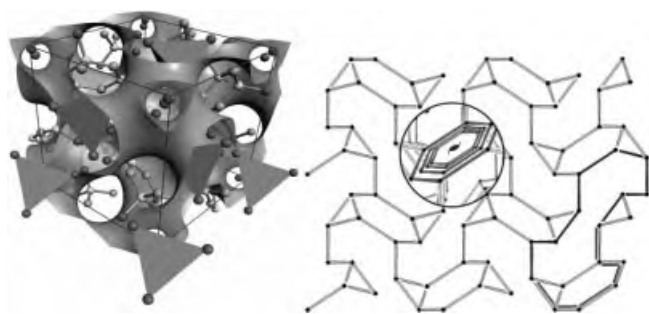


Fig. 7 Crystal structure of the hyperbolically layered oxonitridosilicate oxide $\text{Ce}_4[\text{Si}_4\text{O}_4\text{N}_6]\text{O}$. Left side: The periodic nodal surface (PNS) FYxxx envelops the large tetrahedral cationic complexes $[\text{Ce}_4\text{O}]^{10+}$. Right side: Topological representation of the Si/O/N network structure in $\text{Ce}_4[\text{Si}_4\text{O}_4\text{N}_6]\text{O}$, view along [100]. The O and N atoms are omitted and neighboring tetrahedral centers are directly connected.

$\text{RE}_{(6+x/3)}[\text{Si}_{(11-y)}\text{Al}_y\text{N}_{(20+x-y)}\text{O}_{(1-x+y)}$ with RE = Nd, Er, Yb, or Dy resemble the crystal structure of $\text{Er}_6[\text{Si}_{11}\text{N}_{20}]\text{O}$ [28]. A remarkable result is the identification of $\text{Ce}_{16}\text{Si}_{15}\text{O}_6\text{N}_{32}$ [29] as a defect variant of a perovskite superstructure built up by a condensed network of corner sharing $\text{Si}(\text{O/N})_4$ tetrahedra, SiN_6 octahedra, and Ce^{3+} .

However during these investigations several novel structure types were found as well: In the system Ce-Si-O-N the oxonitridosilicate oxide $\text{Ce}_4[\text{Si}_4\text{O}_4\text{N}_6]\text{O}$ was obtained by the reaction of cerium metal with $\text{Si}(\text{NH})_2$ and SiO_2 at 1560 °C. The cubic structure and the ordering of O and N was determined by single-crystal X-ray diffraction and neutron powder diffraction and it was confirmed by lattice energy calculations using the MAPLE concept. In the solid there are complex cations $[\text{Ce}_4\text{O}]^{10+}$ which are enveloped by a hyperbolic layer structure $[\text{Si}_4\text{O}_4\text{N}_6]^{10-}$ (Fig. 7). This layer is built up by corner sharing Q^3 type SiON_3 tetrahedra. The oxygen atoms of the SiON_3 units are terminally bound to Si, while all nitrogen are bridging two neighboring Si centers. These nitrogen belong to nitridobridges Si-N-Ce. The periodic nodal surface (PNS) FYxxx describes the topological situation of $\text{Ce}_4[\text{Si}_4\text{O}_4\text{N}_6]\text{O}$ very well. This PNS separates the whole structure into two independent spaces. Thus, topologically there is no path from one surface of the PNS to the other. In $\text{Ce}_4[\text{Si}_4\text{O}_4\text{N}_6]\text{O}$ the entire Si-N substructure extends parallel to this PNS and it is situated on one side of the surface, while both the cations $[\text{Ce}_4\text{O}]^{10+}$ and the terminal oxygen atoms of the SiON_3 tetrahedra are positioned on the other side. The bonds Si-O are piercing the surface. Accordingly $\text{Ce}_4[\text{Si}_4\text{O}_4\text{N}_6]\text{O}$ might best be described as the first hyperbolically layered silicate [30].

The oxonitridoaluminosilicates (sialons) $\text{Sr}_3\text{RE}_{10}\text{Si}_{18}\text{Al}_{12}\text{O}_{18}\text{N}_{36}$ with RE = Ce, Pr, Nd were obtained by the reaction of the respective rare earth metals with $\text{Si}(\text{NH})_2$, SrCO_3 , and AlN at temperatures between 1550–1650 °C. The crystal structures of the isotypic sialons were determined by single-crystal X-ray investigations and in the case of $\text{Sr}_3\text{Pr}_{10}\text{Si}_{18}\text{Al}_{12}\text{O}_{18}\text{N}_{36}$ the crystallographic ordering of O

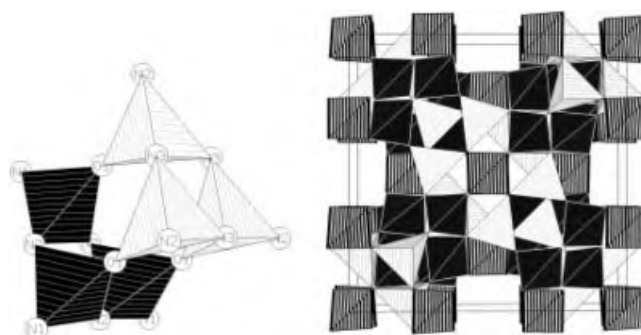


Fig. 8 Crystal structure of the (sialons) $\text{Sr}_3\text{RE}_{10}\text{Si}_{18}\text{Al}_{12}\text{O}_{18}\text{N}_{36}$ with RE = Ce, Pr, Nd, left side: Double three-rings $\text{Si}_3\text{Al}_3\text{O}_3\text{N}_6$ are the characteristic building blocks of the sialon network in $\text{Sr}_3\text{Ln}_{10}\text{Si}_{18}\text{Al}_{12}\text{O}_{18}\text{N}_{36}$, right side: ${}^3_2[(\text{Si}_{18}{}^{[4]}\text{Al}_{12}{}^{[4]}\text{O}_{12}{}^{[2]}\text{N}_{12}{}^{[2]}\text{N}_{24}{}^{[3]})^{24-}]$ network in $\text{Sr}_3\text{Ln}_{10}\text{Si}_{18}\text{Al}_{12}\text{O}_{18}\text{N}_{36}$. The SiON_3 units are depicted as black, the AlON_3 as gray, and the SiN_4 tetrahedra as darkly hatched polyhedra.

and N was investigated with powder neutron diffraction. The three-dimensional sialon network (Fig. 8) is built up from SiON_3 , SiN_4 , and AlON_3 tetrahedra. Surrounded by the sialon network there are large tetrahedral $[(\text{Sr/Ln})_4\text{O}]$ cations. Typical of the crystal structure are double three-rings formed by three SiON_3 and three AlON_3 tetrahedra. Within these units each SiON_3 is connected to an AlON_3 through an O atom. The Si_3N_3 and Al_3N_3 rings of these units exhibit the chair conformation, the resulting four-rings $\text{Al}_2\text{Si}_2\text{N}_2\text{O}_2$ the saddle conformation. Furthermore, the double three-rings are connected through SiN_4 tetrahedra forming the three-dimensional sialon network.

For the first time we performed hardness investigations on sialon single crystals. The investigations exhibit an averaged Vickers hardness for $\text{Sr}_3\text{Pr}_{10}\text{Si}_{18}\text{Al}_{12}\text{O}_{18}\text{N}_{36}$ single crystals of 22.0 GPa. Thus, the determined values are comparable to those of very hard polycrystalline α -sialons and α - Al_2O_3 [31].

The sialon $\text{Sr}_{10}\text{Sm}_6\text{Si}_{30}\text{Al}_6\text{O}_7\text{N}_{54}$ was obtained by the reaction of Sr and Sm with $\text{Si}(\text{NH})_2$, SrCO_3 , and AlN at a maximum reaction temperature of 1600 °C. In the solid a capped double-layer structure of the two-dimensional sialon network is formed by corner sharing SiON_3 , SiN_4 , AlON_3 , and AlN_4 tetrahedra (Fig. 9). The molar ratio T : X (T = Si, Al; X = O, N) for the sialon network exhibits the relatively high value of 0.59. Typically, layered silicates exhibit a degree of condensation in the range 0.25–0.5. Ideal single-layer silicates exclusively contain SiX_4 tetrahedra of Q^3 type and their degree of condensation amounts to Si : X = 2 : 5. For $\text{Sr}_{10}\text{Sm}_6\text{Si}_{30}\text{Al}_6\text{O}_7\text{N}_{54}$ this ratio is 2 : 3.4. A characteristic feature of the sialon network of $\text{Sr}_{10}\text{Sm}_6\text{Si}_{30}\text{Al}_6\text{O}_7\text{N}_{54}$ are large channels running along [001] formed by the strongly corrugated layers A and A'. These layers consist of rings built up by three SiON_3 and SiN_4 tetrahedra. The double layer structure is clearly illustrated by directly connecting the neighboring tetrahedral centers Si and Al (Fig. 9). The Sr^{2+} and Sm^{3+} ions are situated in the voids of the structure of $\text{Sr}_{10}\text{Sm}_6\text{Si}_{30}\text{Al}_6\text{O}_7\text{N}_{54}$.

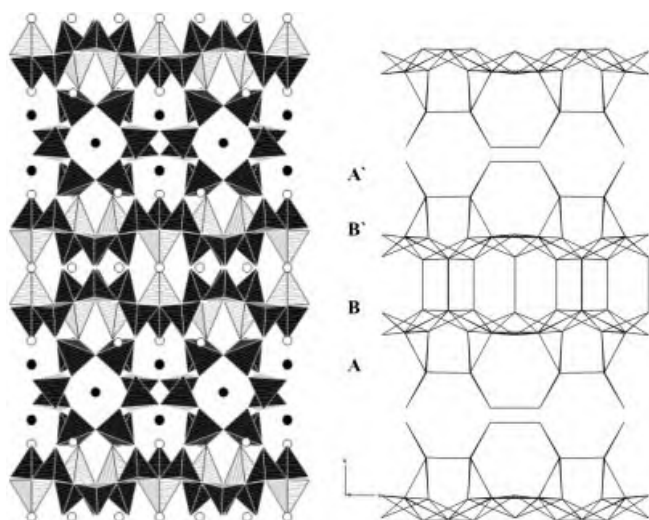


Fig. 9 Double layer structure of the sialon network in $\text{Sr}_{10}\text{Sm}_6\text{Si}_{30}\text{-Al}_6\text{O}_7\text{N}_{54}$ (stacking sequence $\text{ABB}'\text{A}'$); Sr^{2+} white, Sm^{3+} black; left side: polyhedral illustration with SiON_3 and SiN_4 tetrahedra (black) and AlON_3 and AlN_4 (gray); right side: illustration of the directly connected tetrahedral centers Si and Al.

The Sr^{2+} ions are neighboring the weakly corrugated tetrahedral double layers and the Sm^{3+} ions are situated in the large cavities formed by the strongly corrugated layers A and A' (Fig. 9), which are built up by SiON_3 and SiN_4 tetrahedra [32].

Recently, we have investigated $\text{Gd}_3[\text{SiON}_3]\text{O}$, the first oxonitridosilicate oxide with noncondensed SiON_3 tetrahedra, and we have investigated its magnetic and optical properties [33]. The crystal structure derives from the perovskite structure type by a hierarchical substitution ($\text{Ti}^{4+} \rightarrow \text{O}^{2-}$, $\text{O}^{2-} \rightarrow \text{Gd}^{3+}$, $\text{Ca}^{2+} \rightarrow [\text{SiON}_3]^{7-}$).

Nitridophosphates

The incorporation of transition metals or even rare earth elements into pure nitridophosphates seems to be much more difficult as compared to the nitridosilicates. There are some oxonitridophosphates of transition metals known, e.g. $\text{M}^{\text{I}}_3\text{M}^{\text{III}}\text{P}_3\text{O}_9\text{N}$ with $\text{M}^{\text{I}} = \text{Na, K, (Na,K)}$ and $\text{M}^{\text{III}} = \text{Al, Ga, In, Ti, V, Cr, Mn, Fe, (Al,Cr), (Al,V)}$ or $\text{M}^{\text{I}}_2\text{M}^{\text{II}}_2\text{P}_3\text{O}_9\text{N}$ with $\text{M}^{\text{I}} = \text{Na}$ and $\text{M}^{\text{II}} = \text{Mg, Mn, Fe, Co}$. However, all of these compounds do not contain any nitridobridges P-N-M between phosphorus and the transition metals M [34]. In other cases like the isotopic compounds $\text{Cs}_3\text{Fe}_2\text{P}_6\text{O}_{17}\text{N}$ and $\text{Cs}_3\text{Co}_2\text{P}_6\text{O}_{17}\text{N}$ or the series $\text{M}^{\text{I}}_2\text{M}^{\text{II}}\text{P}_3\text{O}_8\text{N}$ with $\text{M}^{\text{I}} = \text{K}$ or Tl and $\text{M}^{\text{II}} = \text{Mg, Mn}$ or Fe nitridobridges P-N-M have not unequivocally been identified as yet [34].

Contrarily, the transition metal nitridosodalites represent a unique and varied group of compounds. Previously, we investigated the nitridosodalites $\text{Zn}_{7-x}\text{H}_{2x}[\text{P}_{12}\text{N}_{24}]\text{Cl}_2$ with $0 \leq x \leq 3$ as well as $\text{M}_{(6+(y/2)-x)}\text{H}_{2x}[\text{P}_{12}\text{N}_{24}]\text{Z}_y$ with $\text{M} = \text{Fe, Co, Ni, Mn}$; $\text{Z} = \text{Cl, Br, I}$; $0 \leq x \leq 4$; $y \leq 2$ [35]. And now we have identified some further representatives of this class of compounds, like $\text{Zn}_8[\text{P}_{12}\text{N}_{24}]\text{X}_2$ with $\text{X} = \text{O, S, Se, Te}$

[36], the partially filled sodalite $\text{Zn}_6[\text{P}_{12}\text{N}_{24}]$, for which hydrogen encapsulation could be proved [37], or even the copper containing oxonitridosodalite $\text{Cu}_{4.8}\text{H}_{3.2}[\text{P}_{12}\text{N}_{18}\text{O}_6]\text{Cl}_2$, whose framework structure is made up from PON_3 tetrahedra [38].

Molecular Precursor Compounds with Nitrido Bridges M-N-Si (M = Ti, Zr, Hf, W, Sn)

In the context of our efforts to synthesize oligonary nonmetal nitrides we have also been interested in developing molecular precursor compounds containing nitridobridges M-N-Si between d-metals like Ti, Zr, or W on one hand and silicon on the other. Especially we are targeting such molecular compounds that subsequently could be transferred into oligonary silicon nitrides by a simple ammonolysis reaction. We preferentially have utilized chlorine as a secondary ligand at the metal or at the silicon atoms that easily can be removed by a simple reaction with ammonia under formation of NH_4Cl .

The titanium complex $\text{Cl}_3\text{Ti}[\text{N}(\text{SiMe}_2\text{Cl})(\text{SiMe}_2\text{NH}_2)]$ (**1**) was obtained by the reaction of 1-chloro-1,1,3,3,3-pentamethyldisilazane (**2**) with TiCl_4 according to equation (4).

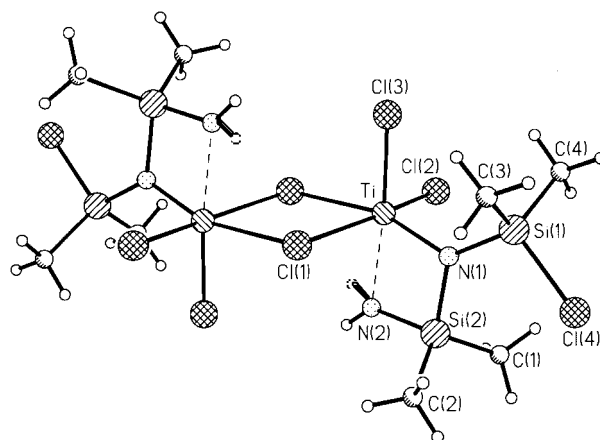


Fig. 10 Structure of $[\text{Cl}_3\text{Ti}(\text{N}(\text{SiMe}_2\text{Cl})(\text{SiMe}_2\text{NH}_2))]_2$ (**1**) in the solid.

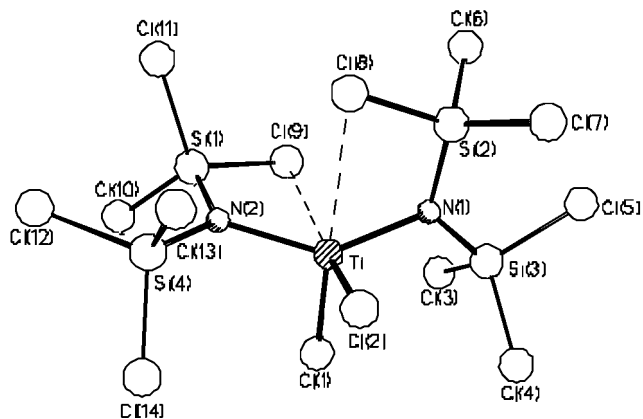
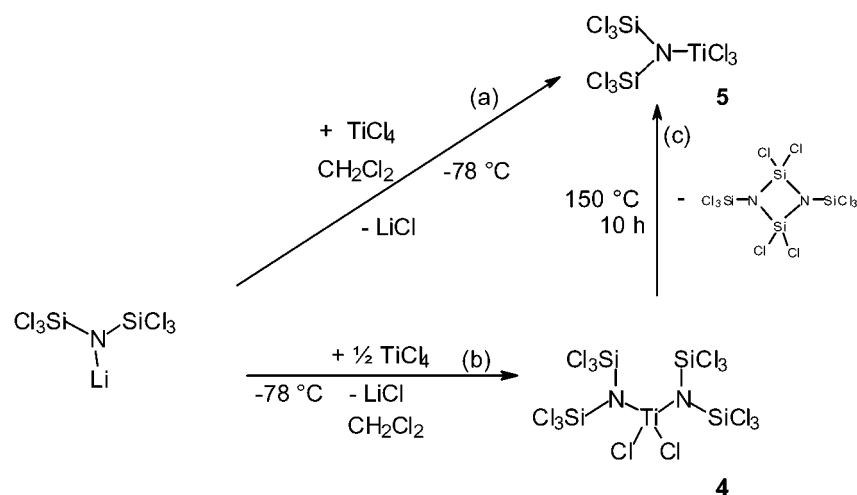
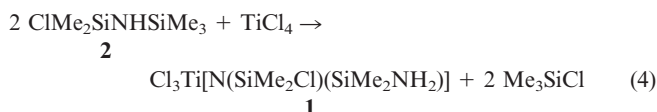


Fig. 11 Structure of $[(\text{Cl}_3\text{Si})_2\text{N}]_2\text{TiCl}_2$ (**4**) in the crystal.



Scheme 1

The disilazane (**2**) previously has been synthesized starting from hexamethyldisilazane (HMDS) and Me_2SiCl_2 . Apparently both reactions are driven by evolution of Me_3SiCl .



According to $[\text{Cl}_3\text{Ti}(\text{N}(\text{SiMe}_2\text{Cl})(\text{SiMe}_2\text{NH}_2))]_2$ complex **1** is dimeric in the solid (Fig. 10). The entire molecule exhibits an inversion center. The titanium atoms are coordinated by four Cl and two N each forming distorted octahedra. Both moieties are connected through the Cl atoms of common edges of both TiCl_4N_2 octahedra.

Four membered rings Ti-N(1)-Si(2)-N(2), which are approximately planar, are the characteristic structural building blocks of both entities. The remaining bonds of Si are saturated by methyl groups and Cl substituents, respectively. Presumably the formation of (**1**) is initiated by elimination of HCl from $\text{ClMe}_2\text{SiNHSiMe}_3$ and TiCl_4 . As a byproduct of this reaction $(\text{NH}_4)_2\text{TiCl}_6$ is formed. Subsequently a second molecule $\text{ClMe}_2\text{SiNHSiMe}_3$ is bonded by the elimination of Me_3SiCl under formation of the four membered ring Ti-N-Si-N. Further addition of HCl and dimerization leads to the formation of (**1**) [39]. Direct reaction of the trisilazane $\text{Cl}_2\text{Si}(\text{NHSiMe}_3)_2$ with TiCl_4 in *n*-pentane leads to the formation of $[\mu\text{-ClTiCl}_2\text{N}(\text{SiMe}_3)\text{SiCl}_2\text{NH}_2]_2$ (**3**), which represents a simple substitutional variant of $[\mu\text{-ClTiCl}_2\text{N}(\text{SiMe}_2\text{Cl})\text{SiMe}_2\text{NH}_2]_2$ (**1**) [40]. Surprisingly both dimeric complexes (**1**) and (**3**) crystallize with quite similar monoclinic lattice constants, and thus they are homeotypic. Currently we investigate, if these N-silylamido titanium chlorides are appropriate molecular precursor compounds for the synthesis of nitrides. Preliminary investigations have indicated, that their ammonolysis followed by a pyrolysis leads to the formation of nanocrystalline TiN in a matrix of amorphous silicon nitride.

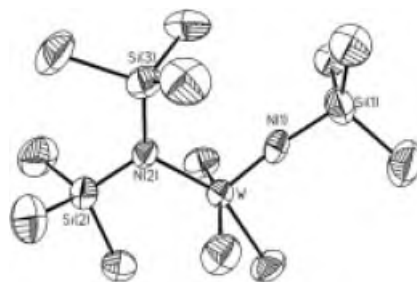


Fig. 12 Structure of $\text{Cl}_3\text{SiN}\equiv\text{W}(\text{Cl}_3)\text{N}(\text{SiCl}_3)_2$ (**6**) in the crystal.

Fully chlorinated N-silyl metal amides and imides

The reaction of hexachlorodisilazanyllithium (Cl_3Si)₂NLi with TiCl_4 selectively leads to the fully chlorinated amides $[(\text{Cl}_3\text{Si})_2\text{N}]_2\text{TiCl}_2$ (**4**) and $(\text{Cl}_3\text{Si})_2\text{NTiCl}_3$ (**5**). The structure of **5** has been deduced by mechanistic considerations and on the basis of the characteristic ¹⁴N and ²⁹Si NMR data. Thus **4** and **5** are formed according to Scheme 1.

The structure of $[(\text{Cl}_3\text{Si})_2\text{N}]_2\text{TiCl}_2$ (**4**) has been elucidated by a single-crystal X-ray structure determination (Fig. 11) [41].

Analogously WCl_6 has been reacted with hexachlorodisilazanyllithium (Cl_3Si)₂NLi, and we obtained the fully chlorinated amide imide $\text{Cl}_3\text{SiN}\equiv\text{W}(\text{Cl}_3)\text{N}(\text{SiCl}_3)_2$ (**6**) according to Scheme 2. The structure has also been elucidated by single-crystal X-ray structure determination (Fig. 12) [42].

Reactions of hexamethyldisilazane (HMDS) with metal chlorides

Recently Seyferth et al. [43] reported about the reaction of hexamethyldisilazane (HMDS) with TiCl_4 , that should lead to a product with the postulated formula $[\text{Me}_3\text{SiNHTiCl}_3]$. However, according to our experience the presence of N-H groups in the product of this reaction seems to be rather unlikely, because usually the reaction between disilazanes and TiCl_4 are initiated by an elimination of HCl. Our de-

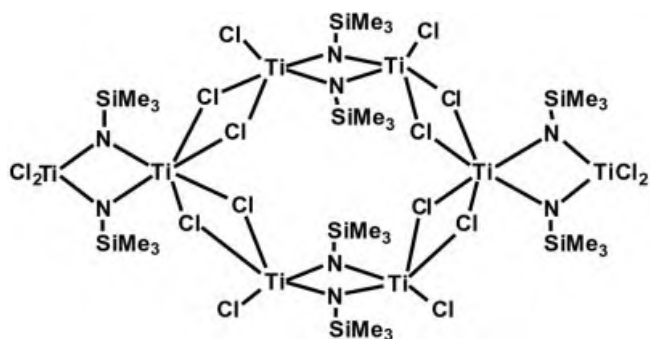


Fig. 13 Structure of the octameric titanium trimethylsilylimido chloride $[\text{Me}_3\text{SiNTiCl}_2]_8$ (**8**).

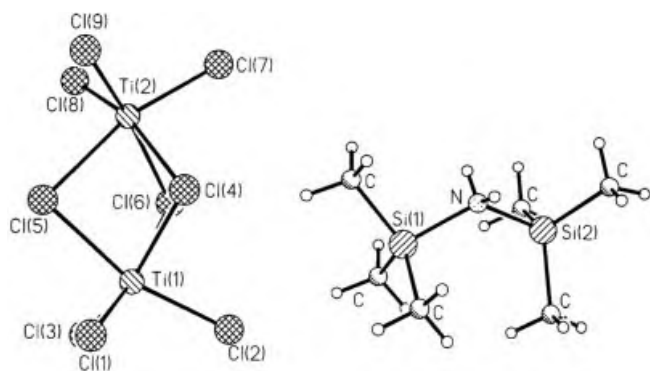
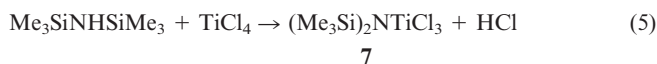


Fig. 14 Structure of cations and anions of the first bis(trimethylsilyl)ammonium salt $[(\text{Me}_3\text{Si})_2\text{NH}_2]^+[\text{Ti}_2\text{Cl}_9]^-$ (**9**) in the crystal.

tailed investigation revealed the true nature of the product from the reaction of HMDS with TiCl_4 : According to equation (5) the intermediate product $[(\text{Me}_3\text{Si})_2\text{NTiCl}_3]$ (**7**) is formed, which by further elimination of Me_3SiCl transforms into **8**.



According to the single-crystal X-ray structure determination $[\text{Me}_3\text{SiNTiCl}_2]_8$ (**8**) occurs in the crystal as an octameric titanium trimethylsilylimido chloride (Fig. 13) [44]. As *Seyferth* et al. already have pointed out, this compound is a valuable precursor compound for the fabrication of thin films of titanium nitride on alumina substrates by a single dip-coat-fire sequence [43].

During our detailed investigations we have identified both $(\text{NH}_4)_2\text{TiCl}_6$ and the hitherto unknown bis(trimethylsilyl)ammonium salt $[(\text{Me}_3\text{Si})_2\text{NH}_2]^+[\text{Ti}_2\text{Cl}_9]^-$ (**9**) as further byproducts of the reaction between HMDS and TiCl_4 . According to the single-crystal X-ray structure determination [44] the protonation of HMDS, that previously has not been described in the literature, causes a significant elongation of the Si-N bond from 173.5 pm (in HMDS) to 186 pm in the cation of **9** (Fig. 14).

Subsequently we were able to identify further chlorides of tetravalent metals that form bis(trimethylsilyl)ammonium salts by the reaction with HMDS as well. In the case of ZrCl_4 a complex chlorotrimethylsilylimido-zirconate

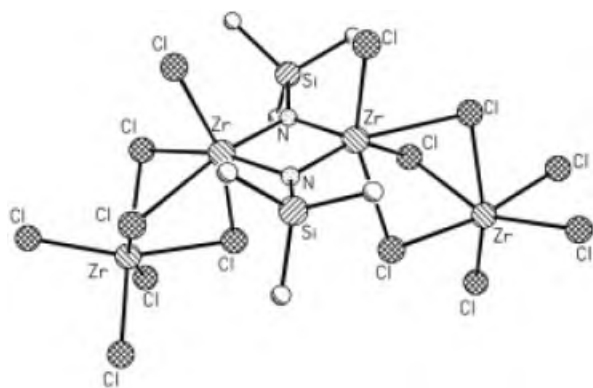


Fig. 15 Structure of the anion of the bis(trimethylsilyl)ammonium salt $[(\text{Me}_3\text{Si})_2\text{NH}_2]^+_2 [(\text{Cl}_3\text{ZrCl}_3\text{Zr}(\text{Cl})(\text{NSiMe}_3))_2]^{2-}$ (**10**) in the crystal.

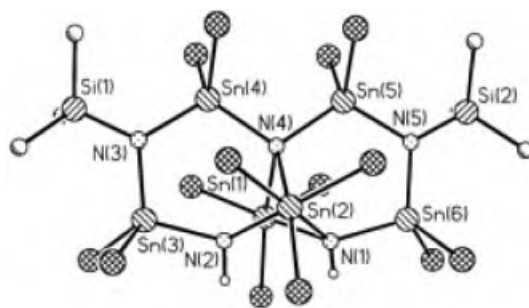
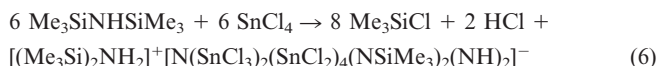


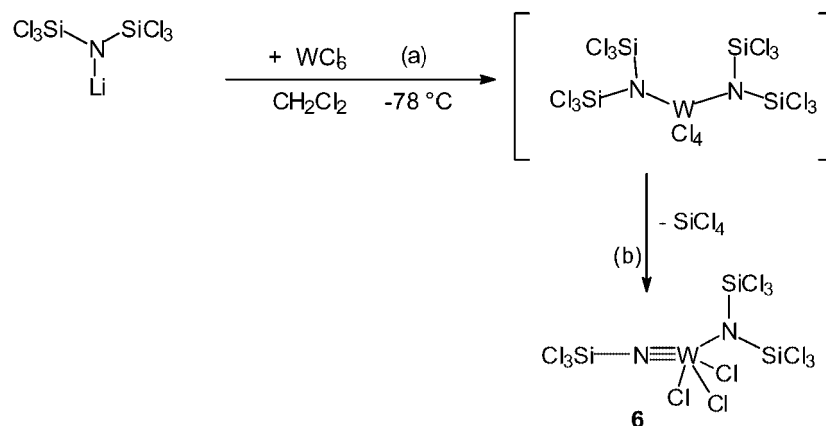
Fig. 16 Structure of the spirocyclic anion of the bis(trimethylsilyl)ammonium salt (**11**), that forms during the reaction of SnCl_4 with HMDS.

with nitridobridges Si-N-Zr is formed with the formula $[(\text{Me}_3\text{Si})_2\text{NH}_2]^+_2 [(\text{Cl}_3\text{ZrCl}_3\text{Zr}(\text{Cl})(\text{NSiMe}_3))_2]^{2-}$ (**10**) (Fig. 15) [44].

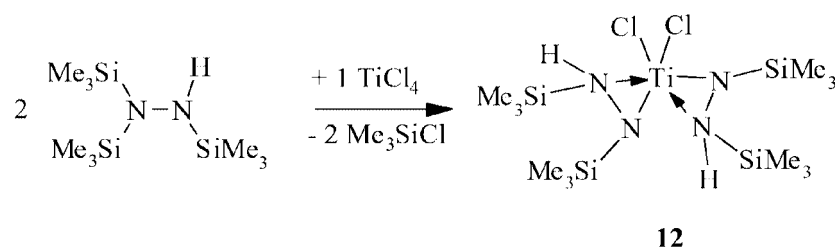
According to equation (6) the analogous reaction of HMDS with SnCl_4 resulted in the formation of a bis(trimethylsilyl)ammonium salt **11** with a completely unexpected anion [44]: The crystal structure analysis reveals a novel spiro anion (Fig. 16) together with the $[(\text{SiMe}_3)_2\text{NH}_2]^+$ ions. The rings of the anion are formed by alternating Sn and N atoms. The resulting distances Sn-N (200 to 229 pm) are comparable to Sn-N single bonds (214 pm). Both NSiMe_3 groups represent fragments of the starting material HMDS. The quaternary nitrogen atoms N(1), N(2), and N(4) carry a formal positive charge (ammonium type) and are not directly bound to Si. Nevertheless, all of them must have been formed by substitution of SnCl_2 and SnCl_3 groups to $\text{Me}_3\text{SiNHSiMe}_3$ under complete elimination of Me_3SiCl during the formation of the spiro anion. Accordingly, HMDS acts as a synthon for nitrogen in the framework of alternating Sn and N atoms of the anion. To the best of our knowledge compound **11** represents the first example containing tetrastannylated nitrogen [44].



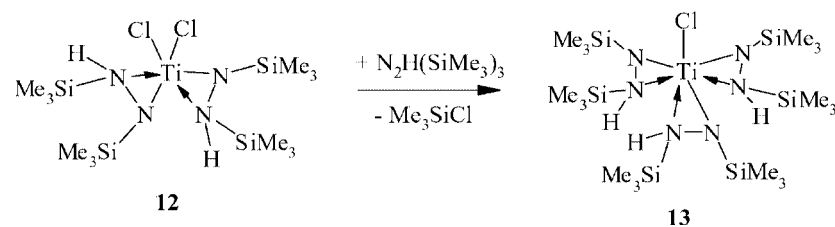
11



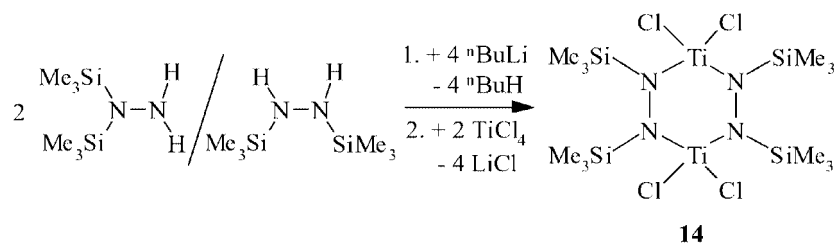
Scheme 2



Scheme 3



Scheme 4



Scheme 5

Silylhydrazido titanium complexes

The silylhydrazido titanium complexes $\text{Cl}_2\text{Ti}[\text{N}_2\text{H}(\text{SiMe}_3)_2]_2$ (**12**), $\text{ClTi}[\text{N}_2\text{H}(\text{SiMe}_3)_2]_3$ (**13**), and $(\text{Cl}_2\text{Ti})_2[\text{N}_2(\text{SiMe}_3)_2]_2$ (**14**) were synthesized by the reaction of the respective (trimethylsilyl)hydrazines with TiCl_4 in solution (Schemes 3 – 5). The reactions were driven by Me_3SiCl elimination or by LiCl elimination after dilithiation of bis-(trimethylsilyl)hydrazine, respectively. According to NMR, mass spectroscopy and X-ray structure determination the products **12** and **13** have been formed by the reaction of

one eq. TiCl_4 with two or three eq. hydrazine. Compound **14** results from the reaction of two eq. TiCl_4 with two eq. hydrazine. According to the results of the single-crystal X-ray diffraction investigation the complexes **12** and **14** exhibit a η^2 -coordination of the hydrazido moiety to titanium. In the crystals of **14** both a chair and a twist form of the six membered rings TiN_2TiN_2 were found representing different donor coordination modes of the hydrazido ligands to titanium. Temperature dependent ^{29}Si NMR investigations indicate that both coordination modes coexist in solution at low temperatures but not at room temperature [45].

Our investigations summarized in this review have been performed between 1996 and 1998 at the University of Bayreuth and from 1998 to 2002 at the University of Munich (LMU). The work extensively has been supported by the Deutsche Forschungsgemeinschaft (DFG) within the Schwerpunktprogramm „Nitridobrücken zwischen Übergangsmetallen und Hauptgruppenelementen“ (SPP 1008, project SCHN377/7) but also by the Gottfried-Wilhelm-Leibniz-Programm (SCHN377/8). Furthermore we are indebted to the Fonds der Chemischen Industrie, Germany, for additional financial support. The authors would like to express their deep gratitude and acknowledgement to the chairmen Prof. K. Dehnicke, Marburg, and Prof. R. Kniep, Dresden, for their superior style of initiation and guidance of this DFG-Schwerpunktprogramm „Nitridobrücken“, and we thank all participants of this program for valuable discussions, many cooperations, and critical comments.

References

- [1] W. Schnick, *Angew. Chem.* **1993**, *105*, 846; *Angew. Chem. Int. Ed. Engl.* **1993**, *32*, 806.
- [2] H.-P. Baldus, M. Jansen, *Angew. Chem.* **1997**, *109*, 338; *Angew. Chem. Int. Ed. Engl.* **1997**, *36*, 328.
- [3] W. Schnick, H. Huppertz, R. Lauterbach, *J. Mater. Chem.* **1999**, *9*, 289.
- [4] W. Schnick, H. Huppertz, *Chem. Eur. J.* **1997**, *3*, 679.
- [5] H. Lange, G. Wötting, G. Winter, *Angew. Chem.* **1991**, *103*, 1606; *Angew. Chem. Int. Ed. Engl.* **1991**, *30*, 1579.
- [6] P. S. Gopalakrishnan, P. S. Lakshminarasimhan, *J. Mater. Sci. Lett.* **1993**, *12*, 1422.
- [7] E. I. Givargizov, in *Current Topics in Materials Science Vol. 1*, North-Holland Publishing Company, **1978**, p. 79.
- [8] a) T. Schlieper, W. Schnick, *Z. Anorg. Allg. Chem.* **1995**, *621*, 1037; b) T. Schlieper, W. Milius, W. Schnick, *Z. Anorg. Allg. Chem.* **1995**, *621*, 1380.
- [9] a) T. Schlieper, W. Schnick, *Z. Anorg. Allg. Chem.* **1995**, *621*, 1535; b) T. Schlieper, W. Schnick, *Z. Kristallogr.* **1996**, *211*, 254.
- [10] H. Huppertz, W. Schnick, *Z. Anorg. Allg. Chem.* **1998**, *624*, 371.
- [11] H. Huppertz, W. Schnick, *Acta Crystallogr.* **1997**, *C53*, 1751.
- [12] H. A. Höpfe, H. Trill, B. D. Mosel, H. Eckert, G. Kotzyba, R. Pöttgen, W. Schnick, *J. Phys. Chem. Solids* **2002**, *63*, 853.
- [13] H. A. Höpfe, H. Lutz, P. Morys, W. Schnick, A. Seilmeier, *J. Phys. Chem. Solids* **2000**, *61*, 2001.
- [14] a) H. Huppertz, W. Schnick, *Angew. Chem.* **1996**, *108*, 2115; *Angew. Chem. Int. Ed. Engl.* **1996**, *35*, 1983; b) H. Huppertz, W. Schnick, *Z. Anorg. Allg. Chem.* **1997**, *623*, 212.
- [15] H. Höpfe, G. Kotzyba, R. Pöttgen, W. Schnick, *J. Mater. Chem.* **2001**, *11*, 3300.
- [16] H. Huppertz, W. Schnick, *Angew. Chem.* **1997**, *109*, 2765; *Angew. Chem. Int. Ed. Engl.* **1997**, *36*, 2651.
- [17] M. Orth, W. Schnick, *Z. Anorg. Allg. Chem.* **1999**, *625*, 551.
- [18] M. Orth, R.-D. Hoffmann, R. Pöttgen, W. Schnick, *Chem. Eur. J.* **2001**, *7*, 2791.
- [19] S. Schmid, W. Schnick, *Z. Anorg. Allg. Chem.* **2002**, *628*, 1192.
- [20] S. Hampshire, in: R. W. Cahn, P. Haasen, E. J. Kramer (Eds.), *Materials Science and Technology*, vol. 5, VCH, Weinheim, **1994**, pp. 119–171.
- [21] R. Metselaar, *J. Eur. Ceram. Soc.* **1998**, *18*, 183.
- [22] P.-O. Käll, J. Grins, M. Nygren, *Acta Crystallogr.* **1991**, *C47*, 2015.
- [23] W. Schnick, *Int. J. Inorg. Mater.* **2001**, *3*, 1267.
- [24] R. Lauterbach, W. Schnick, *Z. Anorg. Allg. Chem.* **1998**, *624*, 1154.
- [25] W. Schnick, H. Huppertz, R. Lauterbach, *J. Mater. Chem.* **1999**, *9*, 289.
- [26] R. Lauterbach, W. Schnick, *Z. Anorg. Allg. Chem.* **2000**, *626*, 56.
- [27] R. Lauterbach, W. Schnick, *Z. Anorg. Allg. Chem.* **1999**, *625*, 429.
- [28] K. Köllisch, H. A. Höpfe, H. Huppertz, M. Orth, W. Schnick, *Z. Anorg. Allg. Chem.* **2001**, *627*, 1371.
- [29] K. Köllisch, W. Schnick, *Angew. Chem.* **1999**, *111*, 368; *Angew. Chem. Int. Ed.* **1999**, *38*, 357.
- [30] E. Irran, K. Köllisch, S. Leoni, R. Nesper, P. F. Henry, M. T. Weller, W. Schnick, *Chem. Eur. J.* **2000**, *6*, 2714.
- [31] R. Lauterbach, E. Irran, P. F. Henry, M. T. Weller, W. Schnick, *J. Mater. Chem.* **2000**, *10*, 1357.
- [32] R. Lauterbach, W. Schnick, *Solid State Sci.* **2000**, *2*, 463.
- [33] H. Höpfe, G. Kotzyba, R. Pöttgen, W. Schnick, *J. Solid State Chem.* **2002**, *157*, 393.
- [34] R. Marchand, W. Schnick, N. Stock, *Adv. Inorg. Chem.* **2000**, *50*, 193.
- [35] a) W. Schnick, J. Lücke, *Angew. Chem.* **1992**, *104*, 208; *Angew. Chem. Int. Ed. Engl.* **1992**, *31*, 213; b) W. Schnick, J. Lücke, *Z. Anorg. Allg. Chem.* **1994**, *620*, 2014; c) W. Schnick, N. Stock, J. Lücke, M. Volkmann, M. Jansen, *Z. Anorg. Allg. Chem.* **1995**, *621*, 987.
- [36] F. Wester, W. Schnick, *Z. Anorg. Allg. Chem.* **1996**, *622*, 1281.
- [37] J. Weitkamp, S. Ernst, F. Cubero, F. Wester, W. Schnick, *Adv. Mater.* **1997**, *9*, 247.
- [38] N. Stock, E. Irran, W. Schnick, *Chem. Eur. J.* **1998**, *4*, 1822.
- [39] R. Buheitel, W. Milius, W. Schnick, *Z. Naturforsch.* **1996**, *51b*, 1141.
- [40] S. Rannabauer, R. Bettenhausen, W. Schnick, *Z. Anorg. Allg. Chem.* **2002**, *628*, 373.
- [41] B. Schwarze, W. Milius, W. Schnick, *Z. Naturforsch.* **1997**, *52b*, 819.
- [42] B. Schwarze, W. Milius, W. Schnick, *Chem. Ber.* **1997**, *130*, 701.
- [43] C. K. Narula, P. Czubarow, D. Seyferth, *Chem. Vap. Deposition* **1995**, *1*, 51.
- [44] R. Bettenhausen, W. Milius, W. Schnick, *Chem. Eur. J.* **1997**, *3*, 1337.
- [45] B. Goetze, J. Knizek, H. Nöth, W. Schnick, *Eur. J. Inorg. Chem.* **2000**, 1849.